ACTA IMEKO
ISSN: 2221-870X
September 2024, Volume 13, Number 3, 1 - 8

Diagnostic investigation of the wall paints conservative state in a hypogeal room of the archaeological park of Baia (Italy)

Paola Cennamo[1], Alessandro De Rosa[1], Roberta Scielzo[1], Massimo Rippa[2], Giorgio Trojsi[1], Elena Chianese[3]

[1] *Department of Humanities, University of Naples Suor Orsola Benincasa, 80132 Naples, Italy*
[2] *Institute of Applied Sciences and Intelligent Systems "E. Caianiello" of CNR, Pozzuoli (Na), Italy*
[3] *Department of Science and Technology, Parthenope University of Naples, 80143 Naples, Italy*

ABSTRACT
The present study investigated the correlation between the degradation processes of cultural heritage and the environmental parameters of the semi-confined site that houses it. The latter is a semi-underground room (*nymphaeum*) found in the Archaeological Park of Baia (Italy) dating back to the third century; it is decorated with marine motifs and painted with frescos techniques from the same period. Relative humidity and temperature were hourly registered, and the collected data were used to derive daily and annual profiles. The effects of microclimate induced degradation were investigated employing various techniques, such as Ion Chromatography for the chemical characterisation of deposits, and Thermography, for the individuation of biological layers. The data obtained showed that the underground environment, partially submerged by rising brackish water, was affected by the presence of biodeteriogens, whose distribution and growth is strongly favoured, above all, by the environmental parameters and by the substrate characteristics. All the data were then cross-referenced to obtain a complete knowledge of the conservation frameworks of the environments, essential to identify the most compatible and effective restoration methodologies to be applied in the conservation of the *nymphaeum*.

Section: RESEARCH PAPER

Keywords: cultural heritage; microclimate; biodeterioration; underground site; efflorescence's chemical characterization

Citation: P. Cennamo, A. De Rosa, R. Scielzo, M. Rippa, G. Trojsi, E. Chianese, Diagnostic investigation of the wall paints conservative state in a hypogeal room of the archaeological park of Baia (Italy), Acta IMEKO, vol. 13 (2024) no. 3, pp. 1-8. DOI: 10.21014/actaimeko.v13i3.1807

Section Editor: Fabio Leccese, Università Degli Studi Roma Tre, Rome, Italy

Received February 27, 2024; **In final form** June 1, 2024; **Published** September 2024

Funding: This research was funded by (ITA) Project PE 0000020 CHANGES – CUP B53C22003780006 NRP Mission 4 Component 2 Investment 1.3, Funded by the European Union - NextGenerationEU.

Corresponding author: Paola Cennamo, e-mail: paola.cennamo@unisob.na.it

1. INTRODUCTION

Due to a range of anthropogenic and environmental threats, conservation of outdoor archaeological sites constitutes a complex challenge [1]. Wind and exposure to sunlight, high humidity and brackish water infiltrations are among the most frequent and insidious causes of decay, as these microclimatic and environmental factors also contribute to the growth of biodeteriogen microorganisms [2]. Such microbial communities range from autotrophic (algae, cyanobacteria) to heterotrophic (fungi, other bacteria) according to the substrate's chemical composition and exposure conditions [3]; ultimately proliferating wherever they can flourish, these organisms may form conspicuous layers called *Biofilm* that cover the surfaces [4], often producing chromatic alterations by interfering with the artificial pigmentation of painted walls or canvas.

Microbial biocenosis can even be more actively harmful to the integrity of artefacts. They can in fact feed on organic materials, such as natural fibers, paint, or wood; alternatively, they can spread over mosaics and frescos, seeping through stone layers along the path opened by moisture penetration, provoking severe damage [5].

Microclimate also contributes to the decay of cultural heritage in less ambiguous ways: a high rate of humidity and temperature, particularly common in hypogeal environments, often results in severe deformation, exfoliation and detachment of plaster or mural paintings [6], [7]; the presence of brackish water, from nearby sea or lagoons, triggers the formation of salt deposits and encrustations, which tampers with stone materials' features [8].

Figure 1. Frontal photo of room SB-E0-R07, taken from the entrance. Biodeterioration is evident, particularly on the back wall and on the ceiling.

The Mercury's Sector of the Archeological Park of Baia's Roman Thermae, near Naples (Italy), is among many outdoor archaeological sites commonly subjected to this type of alterations. Many of the rooms therein represent typical examples of semi-confined spaces, only partially exposed to direct sunlight and dramatically prone to rainwater infiltration. This condition is further exacerbated in the case of rooms located under the ground level, as for the various *nymphaeums* found all around the northern part of Mercury's sector (Figure 1, Figure 2).

In view of the peculiar features and the position these rooms occupy, they were deemed functional part of the thermal complex; location, architectural structure and hydraulic make-up were in fact instrumental in the exploitation of volcanic hot and mineral waters [9]. For such reasons, these spaces were likely half submerged in the past. Water infiltration in some of these environments is correlated to the extensively studied geological phenomenon known as bradyseism. A form of volcanic-related cyclic subsidence, bradyseism consists in the slow uplifting and subsequent lowering of the caldera floor [10]; this geological event represents one of the main sources of degradation for the Baths of Baia archaeological site, as it stands among the direct causes of brackish water infiltration in the underground rooms [11].

A thorough characterization of the conservation state of architectural surfaces, along with the phenomena of degradation that affects them, would not be comprehensive without taking into consideration the environmental context in which they stand.

Microclimate is notably one of the major causes of degradation of outdoor cultural heritage, taking part in both direct and indirect deterioration as in the case of underground sites. For the latter and, in general, for the remote sites, there are many difficulties in microclimate monitoring due to the lack of electric power or telecommunication infrastructure; at present, many efforts are made to provide new devices allowing to exceed these limitations [12].

Figure 2. Frontal photo of the nearby *nymphaeum*, with the clear presence of brackish water on the lining.

The Archaeological site of Baia constitute a notably complex scenario, featuring both weathering and microbial biodeterioration as well as other nuisances such as the abundance of weeds and other plants, and the proximity of the port area and of the Cumana railway [15].

The hypogeal nature of many of the rooms in Baia's Thermae usually ensures a homogeneous internal microclimate, particularly when it comes to temperature, which results only weakly affected by daily variations [6].

The presence of water, whether from moisture, thermal groundwater, or seawater infiltrations, thereby tends to represent the main source of degradation, especially due to its role in promoting the growth of microbial communities.

It is therefore of utmost importance to take the environmental context into consideration when planning adequate conservative strategies to preserve cultural heritage.

A thorough examination of the most influential environmental parameters was carried out, alongside specific analyses on the various forms of alteration affecting the surfaces, in order to inquire the impact of microclimate on the preservation of cultural heritage sites and its strong connection with the diffusion of infesting microbial communities.

In this paper microclimatic monitoring, chemical analyses and biodeteriogens identification were carried out. Chemical analyses were likewise carried out, using a different approach based on the determination of soluble fraction of the saline efflorescence, useful information for the assessment of the presence of mobile species (that is chemical substances that can migrate in or out the wall, depending on their crystallization or solubilization) and for the formation process understanding.

2. MATERIALS AND METHODS

2.1 Site description

The hypogeal space known as SB-E0-R07 (Figure 1), the main subject of the present work, as well as the adjacent nymphaeum (Figure 2), both located in the northern area of the Mercury's sector, constitute a valuable opportunity to describe any potential correlation among the variety of degradation phenomena affecting underground environments. Despite the proximity, these semi-confined spaces present several dissimilarities. Although probably connected, and only located at the short distance of two meters from each other, their respective grounds present different heights due to bradyseism. As a result of this phenomenon, the second chamber has about 20 cm of brackish water on the lining. A further difference lies in the presence of frescos paintings on the north-eastern wall of SB-E0-R07 (Figure 3), whereas the adjacent nymphaeum presents decorations only on the upper frame. These mural paintings date back to around the I or II century A.D., a time framing supported by the massive use of brickwork for the surrounding structures [13], [14].

2.2 Identification of organisms involved in biodeterioration

Biodiversity of the microflora involved in the phenomena of biodeterioration has been previously characterized through Illumina amplicon sequencing, as described in the work by De Luca *et al.* [17]. Meta-barcoding was carried out by choosing the 16S marker for prokaryote taxonomic annotation, and the 18S

Figure 3. Detail of mural painting, partially covered with biofilm. Top is taken with natural light; bottom is fluorescent after exposition to UV light, obtained using an portable UV lamp (395 nm, Eletorot).

marker was similarly selected for eukaryote taxonomic annotation.

2.3 Environmental parameters collection

The environmental parameters of SB-E0-R07 and of the adjacent room were investigated to characterize the ties between microclimate and degradation. Variations of humidity levels and temperature were measured along the horizontal and the vertical axis (external-internal and inferior-superior respectively), for the duration of one year, employing four data logger ORIA© 2 Pack Wireless Thermometer Hygrometer (temperature range -20/60 °C, ±0.5 °C; humidity range 0-99 % RH, ±5 % RH). Data was collected during two weeks per season (on an hourly base), to trace a daily, seasonal, and annual profile. Each datalogger was put in the border area of the room across the horizontal and vertical axis, to ensure an efficient monitoring of the whole environment (points D1-D3 and D2-D4 in Figure 4, respectively).

2.4 Analysis of saline efflorescence

Analysis of saline efflorescence was carried out to investigate the predominance and spatial distribution of detected chemical species. Surface samples were collected at different heights and at different distances from the room entrance (Figure 5), following the vertical and horizontal axis, to highlight the variation in composition of salt species and to verify any correlations with other degradation phenomena. Samples 11 and 12 were collected from the concrete layers in the lower part of the wall on the right; sample 2 was collected from the north wall of the hypogeum, near to the entrance and in an area interested by rainwater infiltration due to the presence of a hole in the ground above. Samples 3 and 6 were collected from the south-east wall, influenced by the thermal water migration from the

Figure 4. Position of the datalogger for the registration of microclimatic parameters.

bordering nymphaeum and from the room below. Samples 1 and 10 were collected in wall sections previously underground. Finally, samples 1, 7, 9, 14, 15 were collected at points interested by a significative presence of biodeteriogens. Before chemical analyses, samples were gently dried, using a drier with silica gel, until a constant weight was reached; an aliquot of each sample was then treated with ultrapure water and sonicated to allow extraction of soluble constituents. Solutions were later filtered using membranes with pores' size of 0.2 mm. Pre-treated samples were finally analyzed using the ion exchange chromatography system Dionex IC-1100 with a double line for anions and cations determination (Cl^-, F^-, Br^-, NO_2^-, NO_3^-, PO_4^{3-}, SO_4^{2-}, $HCOO^-$, CH_3COO^-, $C_2O_4^{-2}$, Na^+, K^+, NH_4^+, Ca^{2+} and Mg^{2+}); compliance method and accuracy were discussed in [16].

2.5 Active Thermography

The thermographic investigations were conducted by dividing the frontal wall into six sections, each individually subjected to heating cycles by air convector, until a temperature increase of about 6 °C was reached. Before and after heating, thermal images of each section were recorded with a 10 Hz frame rate using the LWIR microbolometric camera AVIO TVS500 (spectral range 8–14 μm, FPA 320 × 240 pixels and NETD ~ 50 mK at 25 °C), equipped with a 11 mm focal lens (FOV 39°x29°). The commercial software IRT Analyzer (GRAYESS) was used for real-time temperature monitoring and management of basic parameters. From the acquired frames, by analyzing the temporal trend of the temperature of each pixel, the Thermal Recovery

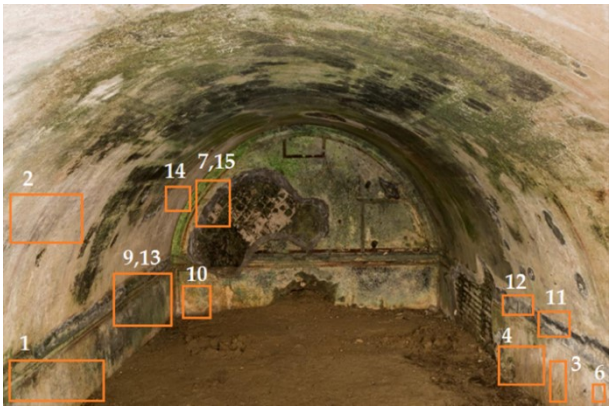

Figure 5. Map of picking spots of salts present in room SB-E0-R07.

Maps (TRMs) of the investigated wall sections were calculated using a home-made MATLAB (R2019b, Math-Works) code. The measurements were made in situ in reflection mode before and after the restoration work was carried out on the wall. Average values for the emissivity of 0.88 in the pre-restoration phase and 0.91 in the post-restoration phase were estimated for the intact area of the wall using an opaque black reference disc and considered in the analysis carried out.

3. RESULTS AND DISCUSSION

3.1 Environmental parameters trends

Data in Figure 6 to Figure 9 showing microclimate parameters' fluctuation in room SB-E0-R07 portray thermal and humidity daily trends as broadly stable. Temperature profile indicate only a 2 °C daily excursion in both the perpendicular and parallel sections of the room, consistently with what's expected in underground spaces [6]. Slightly clearer variations are instead observable in the measurements of humidity rate which, while only varying by about 3 % on the horizontal axis, especially in the cold months, show a more significant shift of 6 % along the vertical axis in all seasons. Observing the hygrometric variations (Figure 6 to Figure 8), decreases in overall values around 2 pm are apparent, with a slow degradation towards the minimum starting at about 12 am. These data are fully reflected by thermal measurements (Figure 7 to Figure 9); in fact, at the same time the humidity rate drops, peak temperature is reached.

This is likely explained by the exposition to sunlight of room SB-E0-R07, which is usually highest between 1 pm and 3 pm, leading to an increase in temperatures and a lowering in humidity, particularly in the areas close to the entrance. After 2 pm, a slow increase in the hygrometric rates is evident and a decrease of the overall temperatures follows, corresponding with the evening time slots. The general stability of indoor temperature and the regularly high relative humidity are surely caused by the influence of thermal water present in the nearby nymphaeum and under room SB-E0-R07, complimented by the hypogeal nature of the whole structure.

3.2 Biodiversity of deteriogens

An intense humidity of up to 97 %, along with mild temperatures only slightly going over 20 °C during summer, promote the proliferation of biodeteriogens on the fresco paintings. The biofilms they form feature different shades of green, as discussed in De Luca *et al.* [17]: each different colors of patina indicates a specific type of microbial community, mostly represented by Cyanobacteria and algae [18].

Cyanobacteria were the dominant phylum in almost all samples, shortly followed by Actinobacteriota and Alphaproteobacteria. The cyanobacteria are fine known settlers of ancient and modern stone monuments, where they constitute a very active and almost omnipresent fraction of the microflora [19].

Previous analyses conducted by De Luca *et al.* [17] indicate that the two nymphaea host profoundly different microbial communities, with approximately only the 8 % of shared taxa. Such an unconformity is likely due to the very different microclimatic environments the two rooms represent. The greater microbial richness of SB-E0-R07, for instance, might be explained by the absence of brackish water, along with the more conspicuous presence of soil near the entrance. Sampling and biomolecular analyses in SB-E0-R07 showed, among others,

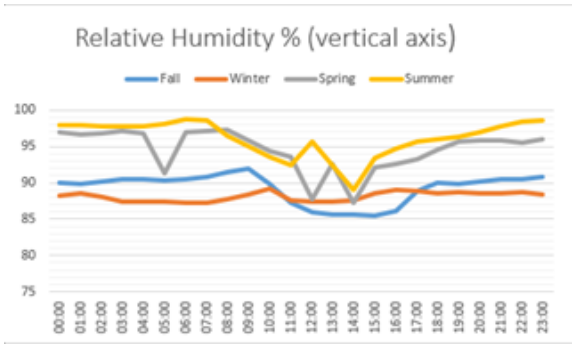

Figure 6. Seasonal trend of hourly relative humidity for the vertical axis.

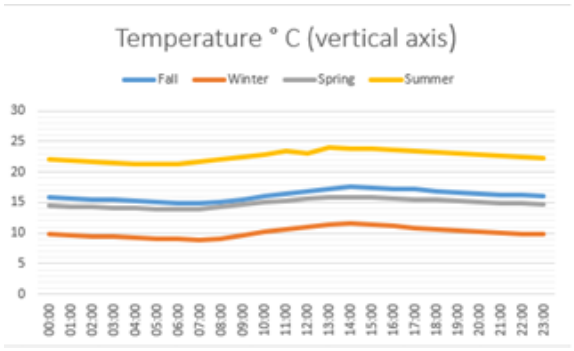

Figure 7. Seasonal trend of hourly temperature for the vertical axis.

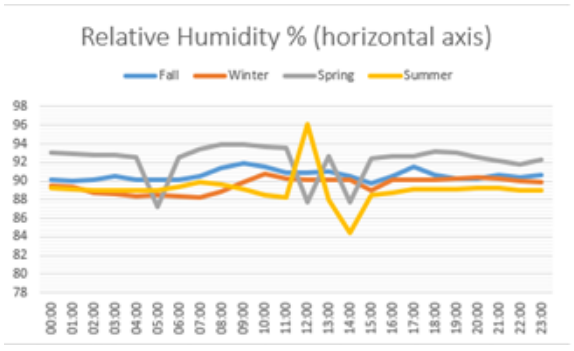

Figure 8. Seasonal trend of hourly relative humidity for the horizontal axis.

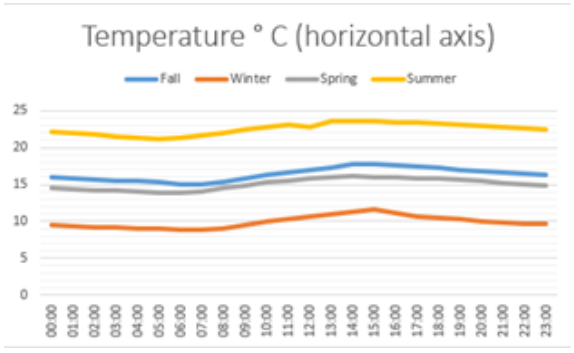

Figure 9. Seasonal trend of hourly temperature for the horizontal axis.

bacterial taxa commonly found in open-air soils such as Rhizobiales, Burkhorderiales and Frankiales. Similarly, analyses on the samples collected from the adjacent nymphaeum highlighted the presence of several marine eukaryotic taxa (i.e. diatoms, dinoflagellates, bivalves). The samples collected on the north-eastern wall of the SB-E0-R07 nymphaeum (Figure 10) tend to vary on a smaller scale: as highlighted in the work by De

Figure 10. North-eastern wall of SB-E0-R07, showing the three sampling spots: 2C, 4C and 5C.

Luca *et al.* [17], Actinobacteriota are prevalent on the exfoliated section, mainly composed of limestone (5C), as opposed to the plasters (2C, 4C); on the other hand, while Cyanobacteria are similarly represented in all samples, Chlorophyta (green algae) seems to only be prevalent among eukaryotes in samples 5C and 2C, both found in the upper regions of the wall.

3.3 Ionic composition of saline efflorescence

The peculiar environmental features and location of the nymphaea, and the resulting infiltration of brackish water from the sea, also led to the formation of encrustations produced by wide range of saline compounds.

In Figure 11 and Figure 12, ionic composition (expressed as percentage) of sample 3 and 6, previously collected from the lower part of the wall adjacent to the nymphaeum, are reported. Sample 3 shows a high level of calcium (Ca^{2+}), attributable to the substrate chemical composition (mostly calcium carbonate).

Additionally, sodium (Na^{+}) and sulphates (SO_4^{2-}) exhibit a comparably high concentration in the analyzed sample. Substantial presence of the latter species can be related to the permeation of thermal water from the adjacent nymphaeum (chemical composition of the water is showed in Figure 13). As confirmed by the massive presence of chloride (Cl^{-}), thermal water is unquestionably of marine nature.

To better understand the considerable presence of sulphates (SO_4^{2-}) and to assess thermal water's contribution to salts deposition, a mass balance was carried out.

In particular, the contribution of sea-salt (expressed as mg of sea salt per gram of sample) was determined by means of the relation [21]:

$$\text{sea salt (mg/g)} = [\text{Cl-}] + 1.47 \times [\text{Na+}].$$

For samples 3 and 6, the input from sea-salt is in the range 1-6 mg/g: these values express an unevenness that is explained by the presence of other sources in addition to the permeation of water. It should be noted that points 3 and 6 were previously interred, so the chemical composition of surface samples may be affected by the chemical species typically found in the soil.

Among the considered samples, 13, 11 and 4 show the highest sea-salt contribution, with values of 325, 39 and 20 mg/g respectively; these samples are all collected from the lower section of the walls and present clear signs of moisture (see Figure 4).

The following relation was used to evaluate the amount of sea salt sulphate (ss-SO_4^{2-}), namely the sulphate of marine origin:

$$\text{ss-}SO_4^{2-}\text{ (mg/g)} = [SO_4^{2-}] - [Na^{+}] \times 0.2516.$$

The non-sea salt sulphate (nss-SO_4^{2-}), namely the sulphate attributable to other sources, was determined through the relation:

$$\text{nss-}SO_4^{2-}\text{ (mg/g)} = [SO_4^{2-}]_{tot} - \text{ss-}SO_4^{2-}.$$

The values of nss-SO_4^{2-} in the considered samples are generally very low, even negative in some cases (samples 1, 9, 13, 14, 15), indicating a loss of sulphates to respect the balance of a seawater sample.

On the contrary, samples 4 and 13 showed very high values (151 and 80 mg/g, respectively), proving that the presence of sulphate is clearly due to other sources. Sulphuric-acid-induced sulphation acting on calcium carbonate substrates might explain the high amount of non-sea-salt sulphates registered in the samples; this phenomenon, caused in large part by pollution in the form of high SO_2 atmospheric concentration [22], leads to the formation of calcium sulphate, a partially soluble compound

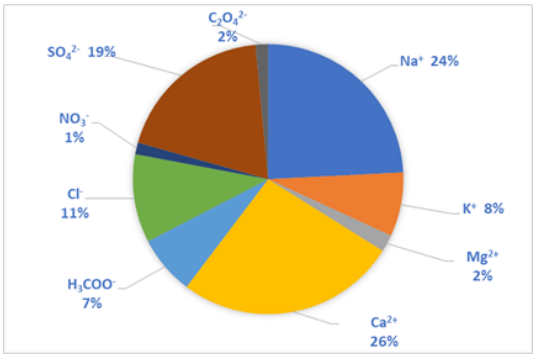

Figure 11. Ionic composition for sample 3, collected from the lower part of the wall adjacent to the *nymphaeum*.

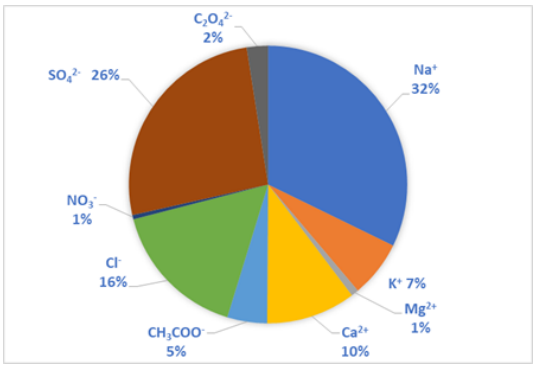

Figure 12. Ionic composition of sample 6, collected from the lower part of the wall adjacent to the *nymphaeum*.

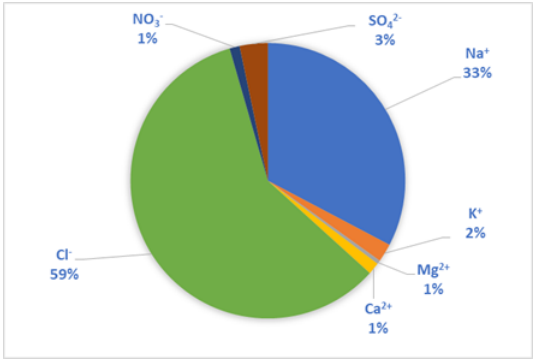

Figure 13. Ionic composition of the thermal water present in the down are of the *nymphaeum*.

Table 1. Ionic composition (expressed as percentage) of deposits collected from walls' surface.

Sample ID	Na^+ %	K^+ %	Mg^{2+} %	Ca^{2+} %	CH_3COO^- %	Cl^- %	NO_3^- %	SO_4^{2-} %	$C_2O_4^{2-}$ %
1	45.989	6.608	0.426	5.731	28.117	4.069	0.941	7.271	0.848
2	4.097	2.898	1.372	25.966	4.484	0.287	0.084	59.299	1.512
3	24.204	7.663	2.041	26.392	7.081	10.590	1.405	19.143	1.481
4	3.351	0.358	0.160	20.673	0.000	4.177	0.173	71.109	0.000
6	32.255	6.602	0.865	10.387	4.633	16.228	0.496	26.069	2.464
7	32.186	10.177	2.176	29.552	15.707	0.223	0.679	8.470	0.830
8	16.406	4.570	3.737	13.821	25.353	2.091	0.284	33.214	0.523
9	19.646	4.942	1.128	38.161	31.841	0.872	1.316	2.094	0.000
10	24.471	24.222	0.507	4.250	29.059	1.530	0.502	15.458	0.000
11	23.366	0.000	0.000	0.388	0.000	0.020	0.020	76.206	0.000
12	23.884	7.734	0.270	6.510	1.805	7.001	0.122	52.675	0.000
13	88.837	1.699	0.330	2.342	3.169	0.428	0.240	2.954	0.000
14	43.917	7.670	1.394	23.614	16.404	0.482	0.601	5.918	0.000
15	36.539	8.204	2.070	38.977	11.431	0.361	0.653	1.764	0.000
16	36.133	0.000	0.528	6.250	45.995	0.747	0.453	9.895	0.000

whose behavior stands among the most common causes of stone deterioration [23].

The presence of other ionic organic compounds as oxalate ($C_2O_4^{2-}$) and acetate (CH_3COO^-) (as reported in Figure 11 and 12) may be attributed to the peculiar environmental conditions of room SB-E0-R07. Specifically, these species are product from biodeteriogen microorganisms and, when highly concentrated, they are heavily involved in the corrosion of stone artefacts [24].

Similar phenomena determine a consequent variation of ions percentage in the composition of salts, even when collected from areas adjacent to the site [25], [26].

As listed in Table 1, there is a great heterogeneity in the chemical composition of the other deposits collected from walls surface. Anyway, some similarities can be highlighted among results in the other samples and data can be correlated with the other observations made; in particular: samples 11 and 12 are characterized by great amounts of sulphate mostly due to the substrate (presence of cement mortars); samples 1, 7, 9, 14, 15 are characterized by the presence of significative amounts of organic ions well related to the presence of biodeteriogens (mainly *Cyanobacteria*); samples 7, 9, 14, 15 are also characterized by great amounts of sodium and calcium related to the influence of water penetration and to the substrate composition.

3.4 Active Thermography analysis: TRMs comparison

Active thermographic analysis was performed to investigate the distribution of the biological patina (biofilm) on the surface of the wall and to compare its state before and after the substrate was restored. The wall area was divided into six sections and the thermographic measurement protocol described in 2.5 was applied to each of them. From the thermal data acquired, the TRMs were calculated following a similar approach to that used in previous works [27], [28].

As a first step, the induced temperature variation ΔT, obtained by heating the surface, was calculated for each pixel of the recorded thermal frames; this was carried out by subtracting the temperature registered after thermal stimulation $T(x, y, 0)$ from the temperature acquired before stimulation $T(x, y, t > 0)$

$$\Delta T(x, y, t > 0) = T(x, y, t > 0) - T(x, y, 0)\,. \quad (1)$$

Subsequently, the TRMs were obtained by analyzing the temporal trend of each pixel (x_P, y_P) and estimating the time they take to recover 50 % of their respective $\Delta T(x, y, t > 0)$. The 50 % threshold represents the value that, according to our results, allows for the greatest variation in estimated recovery times for map pixels. However, choosing other threshold values in the range 40 % - 55 % the results of the analysis are not substantially affected.

As an example of the analysis performed, Figure 14 shows one of the six sections of the wall investigated. The figure shows the two photos of the section taken before (a) and after (b) the restoration work and the corresponding TRMs obtained from the measurements made before (c) and after (d) the intervention. In the TRMs, the grey pixels represent those having a recovery time between 5-30 s and the red ones those above the 30 s threshold, approximately two/three greater times compared to most of the gray ones. From a thermal point of view, the presence of biological patinas (essentially made of water and organic matter) on the wall surface induces an average increase in its specific heat. This increase slows down the heat dissipation process in the areas affected by the patinas, thus resulting in higher thermal recovery times. Accordingly, the red areas present in the maps can be considered those most affected by the presence of local water content due to the biofilm transpiration activity. Therefore, the thermal analyses conducted in the pre-restoration phase made it possible to detect the distribution of the biofilm on the investigated wall and highlighted the area most or least affected.

Comparing the TRMs obtained before and after the intervention, in all the six inspected section of the wall a reduction in the size and recovery times of the red areas was observed, and many red pixels in the pre-intervention maps appear gray in the post-intervention ones. The 'downgrading' of the observed color enabled the identification of the areas of the wall surface where the restoration work was partially or totally successful. It is worth noting that the area of the wall affected by the well visible green biological patina at the top left of Figure 14a induced a recovery time of about 25 s before the restoration work (visible in light gray in Figure 14c) and of about 15 s after the restoration (visible in darker gray in Figure 14d); in both cases, values never exceed the threshold of 30 s set by us and therefore, according to our analysis, the areas affected by green patinas are not directly associated with the higher water content in the wall.

This result highlights an important aspect, namely that the more visibly conspicuous patinas, such as the bottle green (mostly associated with cyanobacteria) and the dark green ones,

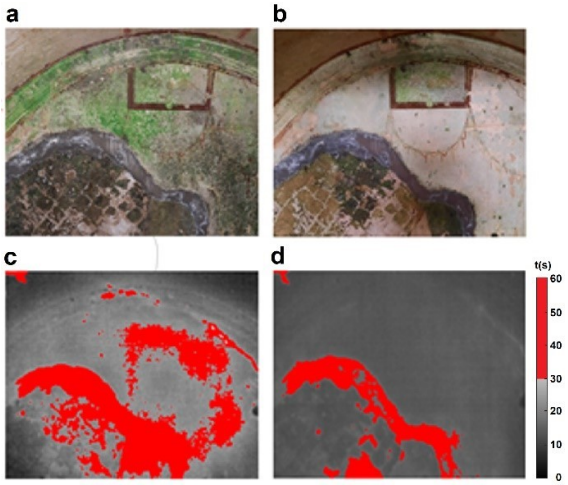

Figure 14. One of the six sections of the SB-E0-R07 room investigated with thermographic analysis: photos of the section before (a) and after (b) a restoration work and corresponding TRMs calculated before (c) and after (d) the intervention.

are not necessarily the most involved in high degrees of water retention. It is in fact likely that the transpiration activity may fluctuate not only between the differently diverse biological patinas present on the wall but also due to their different state of growth. These results represent an argument against a strong direct association between the presence of visibly colored patinas and potential water-induced substrate exfoliation. Although it has been proven that the presence of biofilms on the wall increases general water retention [29] (Figure 14c-d), a varying gradient of water absorption and transport might be easily explained by the differential presence of hydrophobic exudates (EPS) [30], which is in turn dependent on the diversity of the communities involved more than on their abundance. The thermographic analysis thereby not only confirms the wider difference in water retention caused by the disappearance of most of the microbial communities, but it also offers a complementary insight on the ambivalent nature of physio-chemical alteration caused by biodeteriogens.

It's important to underline that this analysis mostly focused on the part of the wall that was still intact, setting the emissivity values relating to this surface in our calculations (reported in the section 2.5). Hence, the recovery times measured for the damaged area at the bottom left in Figure 14a (where a plaster used in a previous restoration is also visible) aren't comparable with those measured on the intact parts of our interest.

4. CONCLUSIONS

The examination of microclimatic parameters and of the chemical composition of saline efflorescence is instrumental for the characterization of deterioration in hypogeal and coastal environments like the roman nymphaea of Baia. High levels of humidity heavily tamper with the integrity of stone surfaces, as confirmed by thermography, while detachments of the preparatory layers of paint and plasters are notably caused by the variations of the physical state of salts. The reduction in cohesion of the original materials provokes, in time, the gradual loss of frescos and decorations, as experimented in-room SB-E0-R07. Salts are also involved in the whitening of the surfaces, further altering the aesthetic impact of the mural paintings.

Thermo-hygrometric conditions, and especially the presence of underground thermal water, on the other side, contributes directly to the manifestation of a broad range of biofilm-forming microorganisms, whose impact for the conservation of stone materials is worryingly well-known. As discussed by De Luca *et al.* [17], the distribution pattern of the nymphaeum's microflora is not only associated with moisture spots, but it is also dependent on the chemical composition of the substrate. The presence of sea eukaryotes, such as marine diatoms and dinoflagellates, seems to be linked to the marine nature of thermal springs, and to the general presence of sea salt in waters therein.

Identification of ionic and biological species, alongside a thorough characterization of the impact of microclimatic and geological influences, offers optimal insight to choose the most context-adequate strategy for conservation. Such an approach also helps to ensure the planning of efficient and durable restorative interventions for the frescoed walls of room SB-E0-R07 [31]. Periodic cleaning of stone artefacts from the diversity of saline and non-saline pollutants, together with the exposure of biofilms to UV-C radiation [32] or the application of essential oils [33] might prove ideal to reduce the biodeterioration phenomena and to secure the preservation of the underground roman nymphaea.

Identifying and quantifying the connection between environmental phenomena, such as high levels of humidity or saline water infiltration, and the microbial colonization of stone materials exposed to such conditions, surely fits the kind of novel multidisciplinary approach that is required for a comprehensive characterization of degradation. The employment of state-of-the-art digital technologies for the measurement of environmental parameters [12] and for the characterization of pollution and deposits [34], [35] will be among the next necessary steps to develop a fully functional workflow, to standardize the analysis of cultural heritage deterioration and make it common practice.

ACKNOWLEDGEMENT

The authors acknowledge Dr. Enrico Gallocchio, archaeological officer of the Archaeological Park of Baia, for the permissions to access the area to conduct the activities of this research.

REFERENCES

[1] K. Vidović, S. Hočevar, E. Menart, I. Drventić, I. Grgić, A. Kroflič, Impact of air pollution on outdoor cultural heritage objects and decoding the role of particulate matter: a critical review, Environmental Science and Pollution Research 29 (2022), pp. 46405-46437.
DOI: 10.1007/s11356-022-20309-8

[2] T. Warscheid, J. Braams, Biodeterioration of stone: a review, International Biodeterioration & Biodegradation 46 (2000), pp. 343-368.
DOI: 10.1016/S0964-8305(00)00109-8

[3] C. Coelho, N. Mesquita, I. Costa, F. Soares, J. Trovao, H. Freitas, A. Portugal, I. Tiago, Bacterial and archaeal structural diversity in several biodeterioration patterns on the limestone walls of the old cathedral of Coimbra, Microorganisms 9 (2021).
DOI: 10.3390/microorganisms9040709

[4] A. De Natale, B. Hay Mele, P. Cennamo, A. Del Mondo, M. Petraretti, A. Pollio, Microbial biofilm community structure and composition on the lithic substrates of Herculaneum Suburban Baths, PLoS ONE 15 (2020).
DOI: 10.1371/journal.pone.0232512

[5] G. Caneva, M. P. Nugari, O. Salvadori, La biologia vegetale per i beni culturali Vol.1: Biodeterioramento e conservazione, Nardini editore, Firenze, 2007, ISBN 9788840441535. [in Italian]

[6] D. Camuffo, Microclimate for cultural heritage: measurement, risk assessment, conservation, restoration, and maintenance of indoor and outdoor monuments, terza edizione. Elsevier. Amsterdam, 2019, ISBN 9780444641069.
[7] C. Danti, M. Matteini, A. Moles, Le pitture murali: tecniche, problemi, conservazione, Centro Di, Firenze, 1990, ISBN 8870381978. [in Italian]
[8] C. Squarciafico, G. Salatino, M. F. La Russa, T. Peluso, L. Basile, F. S. Barbagallo, M. Coppola, A. Macchia, New chemical systems for the removal of calcareous encrustations on monumental fountains: a case study of the Nymphaeum of Cerriglio, Heritage 6 (2023), pp. 6358-6376.
DOI: 10.3390/heritage6090333
[9] S. G. Soutelo, Shall we go "Ad aquas"? Putting roman healing SPAs on the map, Prehistoria y Arquelogia 12 (2019), pp. 151-189.
DOI: 10.5944/etfi.12.2019.25939
[10] G. Leoni, F. Ferrigno, P. M. Guarino, L. Guerrieri, F. Menniti, D. Spizzichino, P. De Martino, M. Di Vito (+3 more authors), Ground motion InSAR monitoring for the protection of Baia Roman Thermae (Naples, Italy) in: Geotechnical Engineering for the Preservation of Monuments and Historic Sites III, first edition, CRC Press, Boca Raton (USA), 2022, ISBN 9781003308867.
DOI: 10.1201/9781003308867
[11] P. Miniero, F. Zevi, Museo Archeologico dei Campi Flegrei, Catalogo Generale Vol I, II, III. Electa, Napoli, 2008, ISBN 9788851005528. [in Italian]
[12] F. Leccese, M. Cagnetti, A. Calogero A., D. Trinca, S. di Pasquale, S. Giarnetti, L. Cozzella, A new acquisition and imaging system for environmental measurements: An experience on the Italian cultural heritage, Sensors 14 (5) (2014), pp. 9290 – 9312.
[13] L. Veronese, Alle origini di una difficile tutela: Amedeo Maiuri e i restauri al parco archeologico delle terme di Baia, Restauro Archeologico 26 (2018). [in Italian]
DOI: 10.13128/RA-23459
[14] G. Di Luca, Cantieri edili e modalità di costruzione nei Campi flegrei di età romana, in Symplegmata in: Symplegmata. Studi di archeologia dedicati a Simona Minichino, pp. 253-282, Giannini Editore, Napoli, 2018, ISBN 9788874319572. [in Italian]
[15] C. Rescigno, La Ferrovia cumana: analisi e sviluppo, Ingegneria ferroviaria: rivista dei trasporti 11 (1986), pp. 781-787. [in Italian]
[16] E. Chianese, G. Tirimberio, A. Riccio, PM2.5 and PM10 in the urban area of Naples: chemical composition, chemical properties and influence of air masses origin, Journal of Atmospheric Chemistry 76 (2019), pp. 151-169.
DOI: 10.1007/s10874-019-09392-3
[17] D. De Luca, R. Piredda, G. Trojsi, P. Cennamo, Close but different: Metabarcoding analyses reveal different microbial communities in ancient Roman nymphaea, Int. Biodeterioration & Biodegradation 181 (2023).
DOI: 10.1016/j.ibiod.2023.105619
[18] W. F. Vincent, Cyanobacteria in: «Encyclopedia of Inland Waters», Elsevier, Amsterdam, 2009, ISBN 012819166X.
[19] C. A. Crispim, C. C. Gaylarde, Cyanobacteria and biodeterioration of cultural heritage: a review, Microbial Ecology 49 (2005), pp. 1-9.
DOI: 10.1007/s00248-003-1052-5
[20] R. De Wit, T. Bouvier, 'Everything is everywhere, but, the environment selects'; what did Baas Becking and Beijerinck really say?, Environmental Biology 8 (2006), pp. 755-758.
DOI: 10.1111/j.1462-2920.2006.01017.x
[21] E. R. Lewis, S. E. Schwarts, Sea Salt Aerosol Production: Mechanisms, Methods, Measurements and Models-A Critical Review, pp. 9–99, American Geophysical Union Washington, DC, 2013, ISBN 9780875904177.
[22] B. Silva, N. Aira, A. Martinez-Cortizas, B. Prieto, Chemical composition and origin of black patinas on granite, Science of the Total Environment 408 (2009), pp. 130-137.
DOI: 10.1016/j.scitotenv.2009.09.020
[23] G. Botticelli, Metodologia di restauro delle pitture murali, self-published, G. Botticelli, 2020, ISBN 8835376386. [in Italian]
[24] A. Duran, M. D. Robador, J. L. Perez-Rodriguez, Degradation of two historic buildings in northern Spain by formation of oxalate and sulphate-based compounds, International Journal of Architectural Heritage 6 (2012), pp. 342-358.
DOI: 10.1080/15583058.2010.551447
[25] M. A. Allan, Manual for the GAW Precipitation Chemistry Programme: Guidelines, Data Quality Objectives and Standard Operating Procedures Vol. CLX, World Meteorological Organization, 2014.
[26] T. Arakaki, S. Azechi, Y. Somada, M. Ijyu, F. Nakaema, Y. Hitomi, D. Handa, Y. Oshiro (+5 more authors), Spatial and temporal variations of chemicals in the TSP aerosols simultaneously collected at three islands in Okinawa, Japan, Atmospheric Environment 97 (2014), pp. 479-485.
DOI: 10.1016/j.atmosenv.2014.04.040
[27] M. Rippa, M.R. Vigorito, M.R. Russo, P. Mormile, G. Trojsi, Active Thermography for Non-invasive Inspection of Wall Painting: Novel Approach Based on Thermal Recovery Maps, J Nondestruct Eval 42, 63 (2023).
DOI: 10.1007/s10921-023-00972-8
[28] M. Rippa, V. Pagliarulo, F. Napolitano, T. Valente, P. Russo, Infrared Imaging Analysis of Green Composite Materials during Inline Quasi-Static Flexural Test: Monitoring by Passive and Active Approaches, Materials 16, 3081 (2023).
DOI: 10.3390/ma16083081
[29] S. McCabe, D. McAllister, P. A. Warke, M. Gomez-Heras, Building sandstone surface modification by biofilm and iron precipitation: emerging block-scale heterogeneity and system response, Earth surface processes and landforms 40 (2015), pp. 112-122.
DOI: 10.1002/esp.3665
[30] L. Schröer, T. De Kock, S. Godts, N. Boon, V. Cnudde, The effects of cyanobacterial biofilms on water transport and retention of natural building stones, Earth surface processes and landforms 47 (2022), pp. 1921-1936.
DOI: 10.1002/esp.5355
[31] P. Cennamo, R. Scielzo, M. Rippa, G. Trojsi, S. Carfagna, E. Chianese, UV-C irradiation and essential-oils-based product as tools to reduce biodeteriorates on the wall paints of the Archeological Site of Baia (Italy), Coatings 13 (2023).
DOI: 10.3390/coatings13061034
[32] P. Cennamo, M. Ebbreo, G. Quarta, G. Trojsi, A. De Rosa, S. Carfagna, P. Caputo, M. M. Castaldi, UV-C Irradiation as a tool to reduce biofilm growth on Pompeii wall paintings, International Journal of Environmental Research and Public Health 17 (2020).
DOI: 10.3390/ijerph17228392
[33] F. Gabriele, R. Ranaldi, L. Bruno, C. Casieri, L. Rugnini, N. Spreti, Biodeterioration of stone monuments: studies on the influence of bioreceptivity on cyanobacterial biofilm growth and on the biocidal efficacy of essential oils in natural hydrogel, Science of the Total Environment 870 (2023).
DOI: 10.1016/j.scitotenv.2023.161901
[34] A. Proietti, L. Liparulo, F. Leccese, M. Panella, Shapes classification of dust deposition using fuzzy kernel-based approaches, Measurement: Journal of the International Measurement Confederation 77 (2016), pp.344-350.
DOI: 10.1016/j.measurement.2015.09.025
[35] A. Proietti, M. Panella, F. Leccese, E. Svezia, Dust detection and analysis in museum environment based on pattern recognition, Measurement: Journal of the International Measurement Confederation 66 (2015), pp.62-72.
DOI: 10.1016/j.measurement.2015.01.019